Biosensors and Bioelectronics 86 (2016) 933–938

Contents lists available at ScienceDirect

Biosensors and Bioelectronics

journal homepage: www.elsevier.com/locate/bios

Electrochemical detection of Nanog in cell extracts via target-induced resolution of an electrode-bound DNA pseudoknot

Jiehua Ma [a,b], Chao Li [a], Yaqin Tao [a], Chang Feng [a], Genxi Li [a,c,*]

[a] State Key Laboratory of Pharmaceutical Biotechnology and Collaborative Innovation Center of Chemistry for Life Sciences, Department of Biochemistry, Nanjing University, Nanjing, 210093 PR China
[b] State Key Laboratory of Reproductive Medicine, Department of Reproductive Health, Nanjing Maternity and Child Health Care Hospital affiliated with Nanjing Medical University, Nanjing, 210004 PR China
[c] Center for Molecular Recognition and Biosensing, School of Life Sciences, Shanghai University, Shanghai, 200444 PR China

ARTICLE INFO

Article history:
Received 23 May 2016
Received in revised form
11 July 2016
Accepted 13 July 2016
Available online 15 July 2016

Keywords:
Electrochemical biosensor
Nanog
Cancer cells

ABSTRACT

Nanog is among the most important indicators of cell pluripotency and self-renew, so detection of Nanog is critical for tumor assessment and monitoring of clinical prognosis. In this work, a novel method for Nanog detection is proposed by using electrochemical technique based on target-induced conformational change of an electrode-bound DNA pseudoknot. In the absence of Nanog, the rigid structure of the pseudoknot will minimize the connection between the redox tag and the electrode, thus reducing the obtained faradaic current. Nevertheless, the Nanog binding may liberate the flexible single-stranded element that transforms the DNA pesudokont into DNA hairpin structure due to steric hindrance effect, thus making the electrochemical tag close to the electrode surface. Consequently, electron transfer can be enhanced and very well electrochemical response can be observed. By using the proposed method, Nanog can be determined in a linear range from 2 nM to 25 nM with a detection limit of 163 pM. Furthermore, the proposed method can be directly used to assay Nanog not only in purified samples but also in complex media (cell extracts), which shows potential applications in Nanog functional studies as well as clinical diagnosis in the future.

1. Introduction

The state of pluripotency, which is regulated very tightly, is one of the most intriguing aspects of cells, since any dysregulation can result in congenital defects, inability to repair damage, or cancer (Allouba et al., 2015). Naong, as one of the most important transcription factors (TFs) involved in pluripotency, has been the great subject of recent interest (Mato Prado et al., 2015) and it has been known that its function is related to cell proliferation, death and determination of cell fate (Sun et al., 2014). It is also known that Nanog is not expressed in most normal adult tissues, but highly expressed in embryonic stem and carcinoma cells (Jeter et al., 2015). Moreover, studies have revealed the contribution of Nanog to stem cell-like phenotypes displayed by many tumors (Ben-Porath et al., 2008; Elsir et al., 2014), thus elevated Nanog level is frequently associated with tumorigenesis, cell invasion and metastasis. So, strong expression of Nanog has been an indicator of high malignant degree, drug resistance and poor clinical outcomes in a variety of cancers (Amaya and Bryan, 2015; Borrull et al., 2012; Lu et al., 2014). Therefore, rapid, sensitive and selective detection of Nanog is critical for tumor assessment, the monitoring of the curative effect of drug intervention, and clinical prognosis (Nagata et al., 2014; Nirasawa et al., 2009).

Currently, the methods for detection of Nanog protein, such as western blots, immunohistochemistry, or electrophoresis mobility shift assay (EMSA) are time-consuming, cumbersome and false negative easily (Lymperopoulos et al., 2010). It has been highly required to develop a simple, sensitive and rapid method to measure Nanog. Therefore, we have designed a DNA pseudoknot for the detection of Nanog in this work. As is shown by Scheme 1, the pseudoknot, a DNA structure, contains two stems (S1 and S2). The S1 stem is designed to be the favorable binding sequence of Nanog, while S2 is designed to be modified with a methylene blue redox tag at its 3′ terminus so as to give electrochemical signal. In the meantime, the background current can be minimized attribute to the relatively rigid structure of the DNA pseudoknot, which may reduce the collisions between the redox tag and the electrode (Wang et al., 2010). Nevertheless, the Nanog binding will break S2, due to the steric hindrance effect resulted from relatively large size of Nanog ($10.5 \times 11.4 \times 6.3$ nm), which may liberate a flexible, single-stranded signaling element that improves electron transfer

* Corresponding author at: State Key Laboratory of Pharmaceutical Biotechnology and Collaborative Innovation Center of Chemistry for Life Sciences, Department of Biochemistry, Nanjing University, Nanjing 210093, PR China.
E-mail address: genxili@nju.edu.cn (G. Li).

http://dx.doi.org/10.1016/j.bios.2016.07.048
0956-5663/

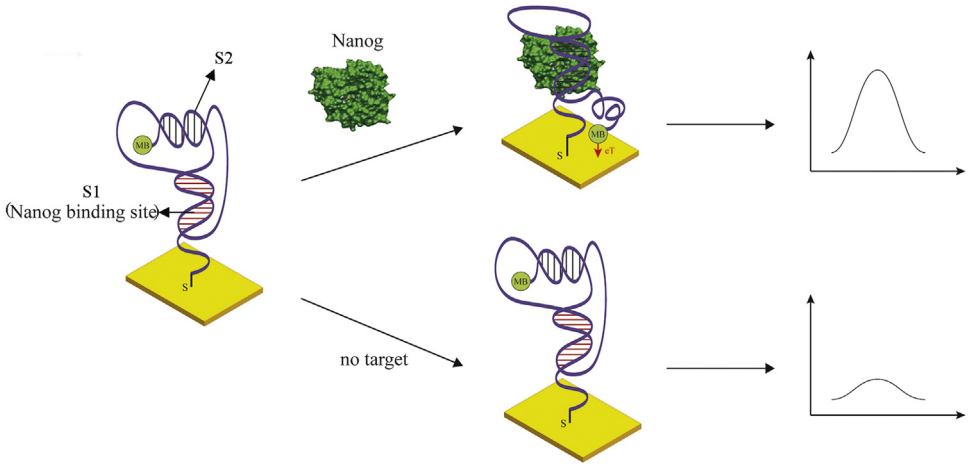

Scheme 1. Schematic illustration of the new method for Nanog detection.

efficiency and increases redox current.

This proposed new method is not only the first report for Nanog detection based on biosensing design, and actually, to our best knowledge, the first report of a new method in contrast to the traditional methods, but it also has several advantages. (1) The detection is simple and rapid. It only needs one-step reaction for about 1 h without onerous washing and processing steps. (2) It is a signal-on electrochemical biosensor architecture that achieves both high signal gain and good stability. (3) The developed method is efficient in thermodynamics for the reason that the Nanog binding site already exists. (4) The design of DNA probe is simplified and the method can be adapted to other protein detection by just replacing the binding sequence. Moreover, by using the proposed assay method, the detection of Nanog in purified samples and in complex media (cell extracts) can be both achieved, so it may have applications in biomedical research as well as clinical diagnosis.

2. Experimental section

2.1. Materials and reagents

The DNA strands with the following sequence used in this work were synthesized and HPLC purified by Sangon Biotechnology Co. Ltd. (Shanghai, China). DNA: 5′-SH-$(CH_2)_6$-TTT TGA CCG ATT ATG TTT AGA TCA GTT CAT AAT CGG TCT TTTTTTTTTTTT CTG ATC T-MB-3′. DNA with nonsense strand: TTT TAT GGA CGG CGA TTT AGA TCA GTT TAC CTG CCG CTT TTTTTTTTTTTT CTG ATC T-MB-3′. Active human Nanog full length protein and Nuclear factor kappa B (NF-κB) p50 were bought from Abcam (Shanghai, China). Tris(2-carboxyethyl)phosphine hydrochloride (TCEP), mercaptohexanol (MCH) and bovine serum albumin (BSA) were obtained from Sigma-Aldrich (Shanghai, China)·H_2O_2 was purchased from Sinopharm Chemical Reagent Co. Ltd. (Shanghai, China). Nuclear protein extraction was conducted using the NE-PER Nuclear and Cytoplasmic Extraction Reagents kit (Thermo Fisher Scientific, USA) according to the manufacturer's protocol. Human Homeobox protein NANOG (NANOG) ELISA kit was bought from Cusabio Biotech Co. Ltd. (Wuhan, China). For all experiments, aqueous solutions purified by Milli-Qplus 185 ultrapure waters system (Barnstead, Bedford, MA) was used. All other chemicals not mentioned here were of analytical reagent grade.

2.2. Preparation of the modified gold electrode

Firstly, the gold electrode (3.0 mm in diameter) was immerged in piranha solution (concentrated H_2SO_4: 30% H_2O_2=3:1) for 15 min to eliminate the adsorbed material, followed by rinsing with distilled water. After that, the electrode was polished with 1 μm and 0.3 μm alumina slurry and sonicated by ultrasonicating in ethanol and distilled water for 10 min in sequence. Subsequently, the electrode was again soaked in piranha solution for 10 min, followed by electrochemical cleaning with 0.5 M H_2SO_4 to remove any remaining impurities. After being dried with mild stream of nitrogen, the electrode was incubated with substrate DNA (0.2 μM in a buffer solution containing 10 mM Tris–HCl, 140 mM NaCl, 1 mM $MgCl_2$, and 5 mM KCl and 1 mM TCEP) for 1.5 h at room temperature. Finally, the electrode was treated with 1 mM MCH for 1 h to obtain well-aligned DNA monolayer.

2.3. Investigation of the binding activity of Nanog and DNA

Nanog was first diluted with buffer (10 mM Tris–HCl, 140 mM NaCl, 1 mM $MgCl_2$, and 5 mM KCl, 1.0% Tween 20) to different concentrations. Then, the prepared DNA modified electrode was immersed in 100 μl of Nanog and reacted at 37 °C for 1 h, followed by washing with buffer. For control experiments, DNA with nonsense strand modified electrode was incubated with 25 nM Nanog, while the DNA with Nanog binding site modified electrode was incubated with 25 nM BSA and NF-κB. Finally, the electrode was ready for electrochemical measurements.

2.4. Preparation of nucleoproteins from cell lines

The MDA-MB-231, Panc-1, SKOV3 and 293T cell lines were purchased from the Institute of Biochemistry and Cell Biology, Chinese Academy of Science. Cells were maintained in DMEM, supplemented with 10% FBS and 1% penicillin streptomycin (pen-strep), under a humidified atmosphere containing 5% CO_2 at 37 °C. Cultures are maintained by the replacement of fresh medium. The medium was renewed every 2–3 days. Cells were harvested with trypsin-EDTA and centrifuge at 500*g* for 5 min, and washed by suspending in the cell pellet with PBS. Then, 2×10^6 cells were transferred to 1.5 ml microcentrifuge tube and brought to nuclear protein extraction. Nuclear protein extraction was conducted using the NE-PER Nuclear and Cytoplasmic Extraction Reagents kit according to the manufacturer's protocol. The extracted nuclear fraction was immediately stored at −80 °C prior to Nanog assay.

2.5. Electrochemical measurements

Electrochemical measurements were performed on a CHI660C Potentiostat (CH Instruments) with a conventional three-electrode

cell at room temperature: a modified gold electrode as the working electrode, a saturated calomel electrode (SCE) as the reference electrode and a platinum wire as the counter electrode. Electrochemical impedance spectroscopy (EIS) was recorded in 5 mM $[Fe(CN)_6]^{3-/4-}$ with 1 M KNO_3. Square wave voltammograms (SWVs) was obtained in 10 mM Tris–HCl buffer (pH 7.0, 140 mM NaCl, 1 mM $MgCl_2$, and 5 mM KCl). The experimental parameters were as follows. EIS: bias potential, 0.225 V; amplitude, 5 mV; frequency range, 0.1 – 10 kHz. SWVs: scan range, – 0.5 to – 0.1 V; step potential, 5 mV; frequency, 15 Hz; amplitude, 25 mV. Then, a stream of nitrogen was blown gently across the surface of the solution in order to maintain the solution anaerobic throughout the experiments. The data were obtained from at least three times of repetition of independent experiment.

3. Results and discussion

3.1. Validation of sensing mechanism

In order to validate the feasibility of the proposed method, EIS has been firstly employed to characterize the stepwise treatment and modification of the electrode surface. EIS can provide prolific information about the change of electrode surface (Huang et al., 2014; Li et al., 2015). The increase in semicircle diameter of EIS spectrum represents the increase of the interfacial charge-transfer resistance. As shown in Fig. 1, little interfacial electron resistance can be observed on the bare gold electrode (curve a). However, after the DNA pseudoknot is immobilized onto the electrode surface, a large semicircle can be observed (curve b), indicating an increase of impedance, due to the reason that the negative electroactive species $Fe(CN)_6^{3-/4-}$ have been electrostatically repelled by the also negatively charged DNA. Furthermore, when Nanog has been captured by the DNA probe, the diameter of the semicircle evidently decreases (curve c), as the released MB-labeled 3′-termini of the probe may dramatically enhance electron transfer (Wang et al., 2015, 2016). Therefore, EIS studies have confirmed the step-by-step modification of the electrode surface. Meanwhile, the experimental may also prove the high affinity of Nanog with the designed DNA pseudoknot immobilized onto the electrode surface.

Fig. 2 depicts the square wave voltammograms (SWV) obtained upon analyzing the Nanog and those obtained in a series of control experiments. As is shown in Fig. 2e, in the presence of 25 nM Nanog, a typical redox peak of MB is observed in the SWV at around – 0.22 V. However, in the absence of Nanog or Nanog binding sequence, only small SWV peaks can be observed (Fig. 2a-d). Such comparison confirms that interference of all the control species can be ignored and the selectivity of our method is satisfactory.

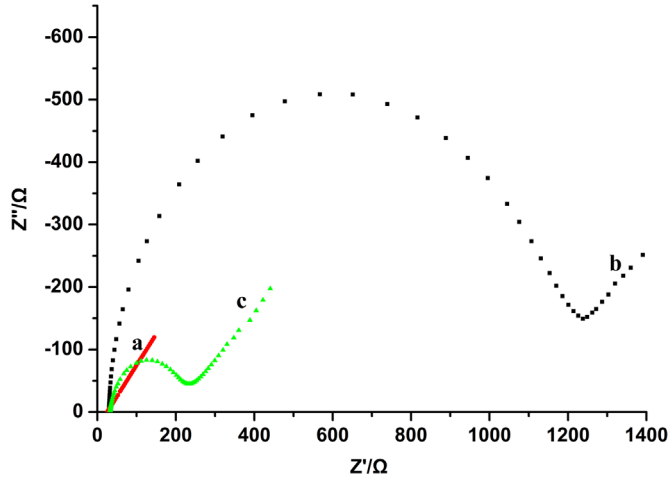

Fig. 1. Nyquist diagrams corresponding to (a) the bare gold electrode, (b) the DNA pseudoknot modified electrode, (c) the DNA pseudoknot modified electrode after being treated with 25 nM Nanog. Electrochemical species: 5 mM $Fe(CN)_6^{3-/4-}$. Biasing potential: 0.224 V. Amplitude: 5 mV. Frequency range: 0.1 Hz to 10 kHz.

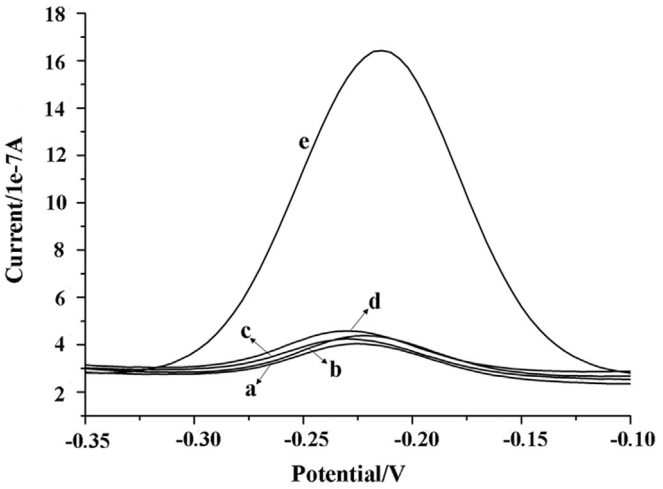

Fig. 2. SWVs obtained at the DNA pseudoknot modified electrode for the cases (a) in the absence of Nanog binding sequence, (b) blank, (c) 25 nM BSA, (d) 25 nM NF-κB and (e) 25 nM Nanog. Tris–HCl solution is used as the blank control.

3.2. Optimization of experimental conditions

Although the binding specificities of Nanog have been demonstrated before, the previous studies cannot offer insights into the influence of environmental factors on the Nanog activity. In this work, to obtain a better assay performance, we have conducted experiments in different experimental conditions by monitoring the obtained SWV response. Firstly, we have optimized the length of poly T loop, since it is the key factor for the target-induced allosterism. If the poly T chain is too short, it cannot form S2. Nevertheless, if the poly T chain is too long, it cannot well respond to the target binding. According to the maximal length of the nucleotide extension (0.5 nm per nucleotide), poly-14T is estimated to be the optimum length which just can form a tight loop. To validate the estimation, we have used 8T to 17T DNA modified electrode for the comparison. As shown in Fig. 3, the results are consistent with our expectations that 14T DNA strand can efficiently obtain high signal with low background. Secondly, the surface density of the DNA pseudoknot has been optimized by varying the concentration of DNA pseudoknot employed for surface modification of the working electrode. As is shown by Fig. S3, an intermediate concentration, namely 0.2 μM, can provide sufficiently high signal readout with no apparent steric hindrance for Nanog/DNA interaction, so this concentration is adopted to modify the working electrode for Nanog detection. Finally, experimental results reveal that the interaction taken place at 37 °C in the buffer with pH 7.4 for 1 h is the best (Fig. S4), so these conditions are used in the following experiments.

3.3. Quantitive detection of Nanog

As shown in Fig. 4A, the proposed new method has been employed to assay the Nanog protein with different concentrations. It can be observed that the SWV response increases along with the increasing concentration of Nanog in the range from 0 to 25 nM. This is certainly reasonable, since more Nanog will result in the release of increased amount of MB onto the electrode surface.

Please cite this article as: Ma, J., et al., Biosensors and Bioelectronics (2016), http://dx.doi.org/10.1016/j.bios.2016.07.048

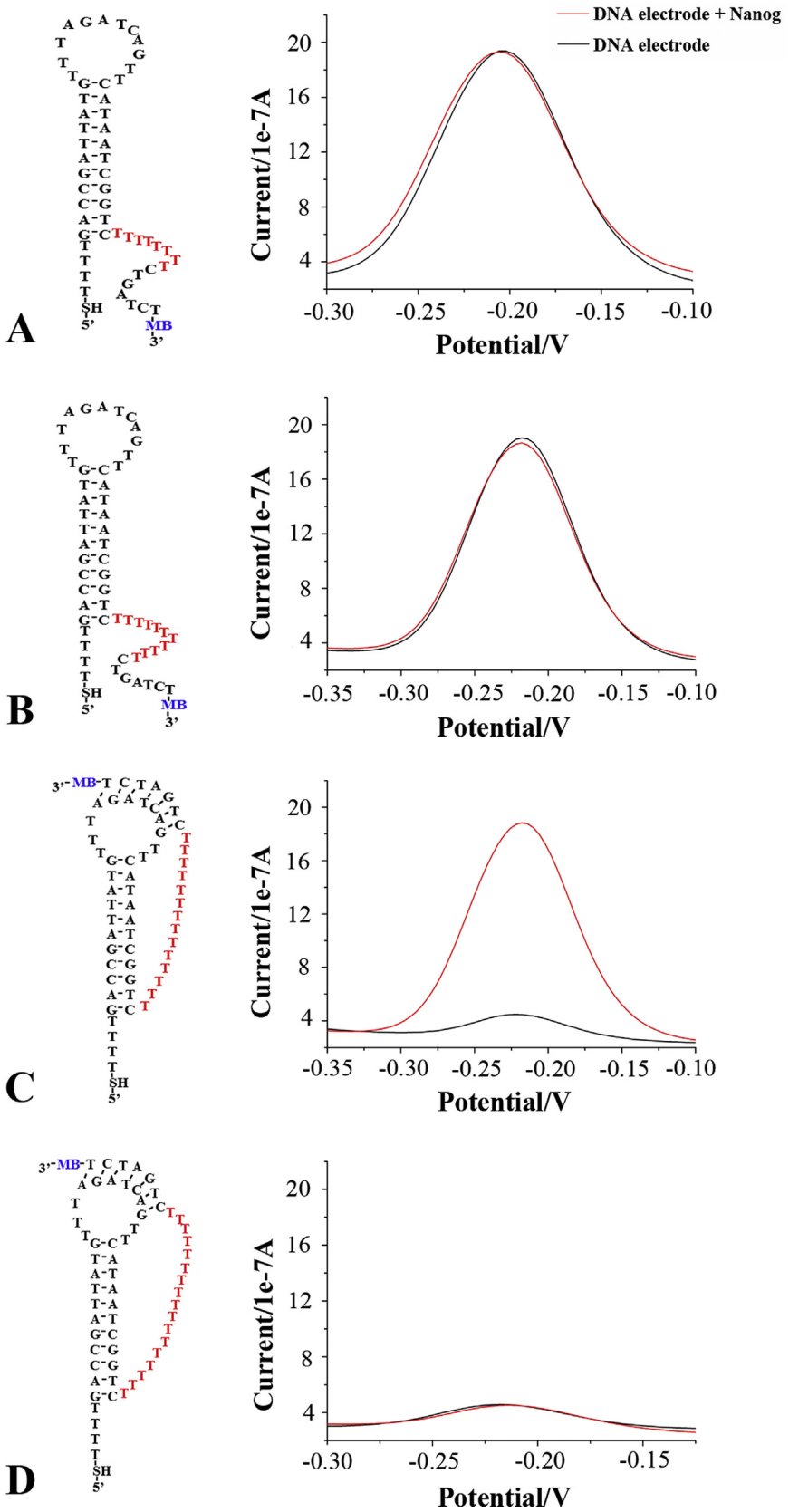

Fig. 3. The optimization of the DNA pseudoknot structure. The change of SWV response (DNA electrode+25 nM Nanog) and background (DNA electrode) upon different poly-T probe: (A) poly-T8, (B) poly-T11, (C) poly-T14 and (D) poly-T17.

Please cite this article as: Ma, J., et al., Biosensors and Bioelectronics (2016), http://dx.doi.org/10.1016/j.bios.2016.07.048

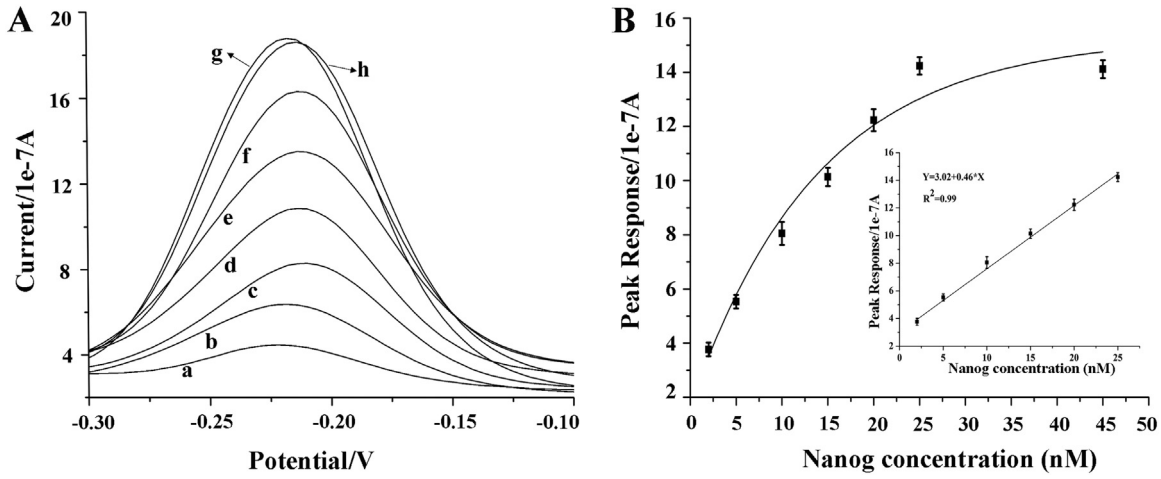

Fig. 4. (A) SWVs corresponding to the analysis of different concentrations of Nanog. The concentrations of Nanog for the curves (a) to (h) are 0, 2, 5, 10, 15, 20, 25 and 45 nM, respectively. (B) Calibration curve corresponding to (A). Inset shows the linear relationship between the peak current and the Nanog concentration. The error bars represent the standard deviation from the average (n=3).

Fig. 4B shows a linear dependence between the SWV peak current and the concentration of Nanog from 2 to 25 nM. For each concentration of Nanog, the measurements have been repeated for at least three times independently. The linear regression equation is determined to be $y=3.02+0.46\ x$ ($R^2=0.998$), where x is the concentration of Nanog and y is the SWV peak response. Furthermore, the detection limit has been calculated as 163 pM by the interpolation of the mean plus three times the standard deviation of the zero standards (Centi et al., 2007). Since the traditional methods (western blots, immunohistochemistry, and electrophoresis mobility shift assay) are semi-quantitative, and our method can be comparable with the recently reported enzyme-linked immunosorbent assay (ELISA) (Rios et al., 2012; Shen et al., 2014), especially in terms of simplicity and performing time (Table S1), the new method proposed in this work will have potential applications in the future.

3.4. Evaluation of Nanog in cancer cells

In order to examine the ability of the proposed method for real samples, cell extracts of MDA-MB-231, Panc-1, SKOV3 and 293T cells have been prepared, and the Nanog protein has been tested to demonstrate the expression difference between cancerous and normal cell lines. As shown in Fig. 5, low signal is observed for 293T cells, indicating the rather low expression of Nanog in 293T cells. However, compared with 293T cells, the peak current apparently increases for MDA-MB-231, Panc-1 and SKOV3 cells, suggesting overexpression of Nanog in cancer cells. Therefore, the experimental results can clearly show the expression difference of Nanog between cancer cell and normal cell, and this new method proposed in this work may be of great value for the detection of Nanog protein complex in biological samples.

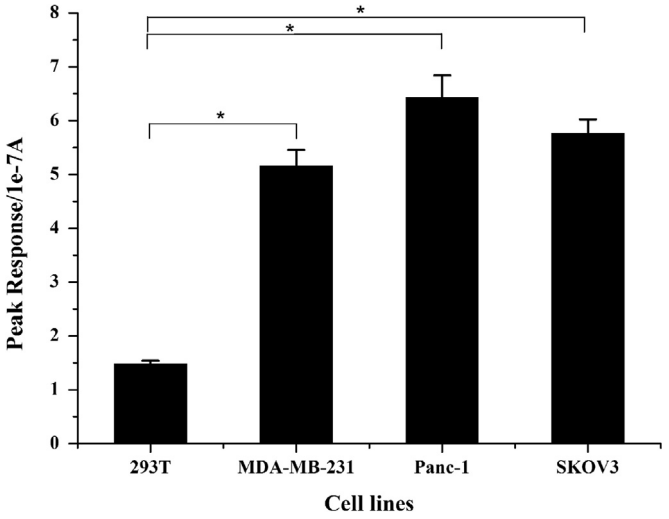

Fig. 5. SWV peak response obtained at the DNA pseudoknot modified electrode for analyzing Nanog from 293 T, MDA-MB-231, Panc-1 and SKOV3 cells. The error bars represent the standard deviation from the average (n=3). *: $P<0.05$.

4. Conclusions

In summary, we have herein reported an electrochemical biosensor for the detection of Nanog, based on target-induced conformation change in an electrode-bound DNA pseudoknot. This new method has also been demonstrated to be able to detect Nanog protein in cell extracts. Moreover, our method may offer several notable advantages than the traditional methods. (1) It is simple and rapid, which only needs one-step reaction for about 1 h. (2) It has low detection limit and wide range with a signal-on performance. (3) It is efficient in thermodynamics, since the protein binding site already exists. (4) It is easy to be versatile, since the method can be adapted to other proteins by just replacing the binding sequence. Therefore, the proposed method may have great potential applications in the future.

Acknowledgments

This work is supported by the National Natural Science Foundation of China (Grant Nos. 81501239, 21235003), and the Fundamental Research Funds for the Central Universities (Grant No. 021414380001).

Appendix A. Supplementary material

Supplementary data associated with this article can be found in the online version at http://dx.doi.org/10.1016/j.bios.2016.07.048.

References

Allouba, M.H., ElGuindy, A.M., Krishnamoorthy, N., Yacoub, M.H., Aguib, Y.E., 2015. NaNog: A pluripotency homeobox (master) molecule. Glob. Cardiol. Sci. Pract. 2015 (3), 36.

Amaya, C.N., Bryan, B.A., 2015. Enrichment of the embryonic stem cell reprogramming factors Oct4, Nanog, Myc, and Sox2 in benign and malignant vascular tumors. BMC Clin. Pathol. 15, 18.

Ben-Porath, I., Thomson, M.W., Carey, V.J., Ge, R., Bell, G.W., Regev, A., Weinberg, R. A., 2008. An embryonic stem cell-like gene expression signature in poorly differentiated aggressive human tumors. Nat. Genet. 40 (5), 499–507.

Borrull, A., Ghislin, S., Deshayes, F., Lauriol, J., Alcaide-Loridan, C., Middendorp, S., 2012. Nanog and Oct4 overexpression increases motility and transmigration of melanoma cells. J. Cancer Res. Clin. Oncol. 138 (7), 1145–1154.

Centi, S., Tombelli, S., Minunni, M., Mascini, M., 2007. Aptamer-based detection of plasma proteins by an electrochemical assay coupled to magnetic beads. Anal. Chem. 79 (4), 1466–1473.

Elsir, T., Edqvist, P.H., Carlson, J., Ribom, D., Bergqvist, M., Ekman, S., Popova, S.N., Alafuzoff, I., Ponten, F., Nister, M., Smits, A., 2014. A study of embryonic stem cell-related proteins in human astrocytomas: identification of Nanog as a predictor of survival. Int. J. Cancer 134 (5), 1123–1131.

Huang, Y., Li, H., Gao, T., Liu, X., Li, G., 2014. A sensitive method for protein assays using a peptide-based nano-label: Human glypican-3 detection for hepatocellular carcinomas diagnosis. Analyst 139 (15), 3744–3747.

Jeter, C.R., Yang, T., Wang, J., Chao, H.P., Tang, D.G., 2015. Concise Review: NANOG in Cancer Stem Cells and Tumor Development: An Update and Outstanding Questions. Stem Cells (Dayt., Ohio) 33 (8), 2381–2390.

Li, H., Huang, Y., Yu, Y., Li, W., Yin, Y., Li, G., 2015. Peptide-based method for detection of metastatic transformation in primary tumors of breast cancer. Anal. Chem. 87 (18), 9251–9256.

Lu, X., Mazur, S.J., Lin, T., Appella, E., Xu, Y., 2014. The pluripotency factor nanog promotes breast cancer tumorigenesis and metastasis. Oncogene 33 (20), 2655–2664.

Lymperopoulos, K., Crawford, R., Torella, J.P., Heilemann, M., Hwang, L.C., Holden, S. J., Kapanidis, A.N., 2010. Single-molecule DNA biosensors for protein and ligand detection. Angew. Chem. (Int. ed. Engl.) 49 (7), 1316–1320.

Mato Prado, M., Frampton, A.E., Stebbing, J., Krell, J., 2015. Gene of the month: NANOG. J. Clin. Pathol. 68 (10), 763–765.

Nagata, T., Shimada, Y., Sekine, S., Hori, R., Matsui, K., Okumura, T., Sawada, S., Fukuoka, J., Tsukada, K., 2014. Prognostic significance of NANOG and KLF4 for breast cancer. Breast Cancer (Tokyo, Jpn.) 21 (1), 96–101.

Nirasawa, S., Kobayashi, D., Tsuji, N., Kuribayashi, K., Watanabe, N., 2009. Diagnostic relevance of overexpressed Nanog gene in early lung cancers. Oncol. Rep. 22 (3), 587–591.

Rios, A., Zougagh, M., Avila, M., 2012. Miniaturization through lab-on-a-chip: Utopia or reality for routine laboratories? A review. Anal. Chim. acta 740, 1–11.

Shen, J., Li, Y., Gu, H., Xia, F., Zuo, X., 2014. Recent development of sandwich assay based on the nanobiotechnologies for proteins, nucleic acids, small molecules, and ions. Chem. Rev. 114 (15), 7631–7677.

Sun, A.X., Liu, C.J., Sun, Z.Q., Wei, Z., 2014. NANOG: a promising target for digestive malignant tumors. World J. Gastroenterol. 20 (36), 13071–13078.

Wang, J., Shen, M., Cao, Y., Li, G., 2010. Switchable "On-Off" electrochemical technique for detection of phosphorylation. Biosens. Bioelectron. 26 (2), 638–642.

Wang, T., Zhang, Z., Li, Y., Xie, G., 2015. Amplified electrochemical detection of mecA gene in methicillin-resistant Staphylococcus aureus based on target recycling amplification and isothermal strand-displacement polymerization reaction. Sens. Actuators B-Chem. 221, 148–154.

Wang, X., Liu, L., Zheng, W., Chen, W., Li, G., Sun, W., 2016. Electrochemical behaviors of myoglobin on graphene and Bi film modified electrode and electrocatalysis to trichloroacetic acid. Int. J. Electrochem. Sci. 11 (3), 1821–1830.

Please cite this article as: Ma, J., et al., Biosensors and Bioelectronics (2016), http://dx.doi.org/10.1016/j.bios.2016.07.048